Relativistic dynamics of Qqq systems

E. F. Suisso

Dep. de Física, Instituto Tecnológico da Aeronáutica, Centro Técnico Aeroespacial, 12.228-900, São José dos Campos, SP, Brazil

J. P. B. C. de Melo

Instituto de Física Teórica, Universidade Estadual Paulista, 01405-900, São Paulo, SP, Brazil

T. Frederico

Dep. de Física, Instituto Tecnológico da Aeronáutica, Centro Técnico Aeroespacial, 12.228-900, São José dos Campos, SP, Brazil

The bound state of constituent quarks forming a Qqq composite baryon is investigated in a QCD-inspired effective light-front model. The light-front Faddeev equations are derived and solved numerically. The masses of the spin 1/2 low-lying states of the nucleon, Λ^0, Λ_c^+ and Λ_b^0, are found and compared to the experimental data. The data are qualitatively described with a flavor independent effective interaction.

I. INTRODUCTION

One major task in strong interaction physics is the calculation of the wave function and the spectrum of the hadrons from quantum chromodynamics (QCD) [1]. Phenomenological dynamical models that retain the low-energy physics of QCD, and relate different observables are still of interest as long as they allow us to expose the nonperturbative properties of QCD. One possibility to model the quark dynamics within a relativistic framework is to use the light-front dynamics in a truncated Fock space, which yields a wave-function covariant under kinematical boosts [2,3]. In general, the light-front Fock-state truncation is stable under kinematical boost transformations [4].

A light-front QCD-inspired model was recently applied to the pion and other mesons [5,6]. It was able to describe the pion structure as well as the masses of the vector and pseudoscalar mesons. This effective model, the $\uparrow\downarrow$ model [5], has two components in the interaction: a contact term and a Coulomb-type potential. The contact term is essential to collapse the constituent quark-antiquark system to form the pion, while the vector meson is dominated by the Coulomb-type potential. In this model the vector meson corresponds to a weakly bound system of constituent quarks. The model has no confinement, and the spin does not play a dynamical role after than justifying the contact term from the hyperfine interaction. However, the contact term was able to embrace the physical scale brought by the pion mass and from that the masses of the other pseudoscalar and vector mesons were calculated [6]. The flavor independence of the interaction was assumed, and the model reproduced fairly well the data, despite its simplicity.

Here we report a nonperturbative calculation of the flavor dependence of the masses of some baryons, extending the concepts coming from the $\uparrow\downarrow$ model applied previously only to mesons [5,6]. In this work, we show that the flavor independence of the effective interaction still holds for baryons,

by studying the spin 1/2 low-lying states of the nucleon, Λ^0, Λ_c^+ and Λ_b^0. To get insight on the complex three-quark relativistic dynamics in this first study of the Qqq system within the light-front framework, we use only the contact interaction, which brings the physical scale of the ground state of the nucleon, while the spin is averaged out. The effect of the long-range Coulomb-type interaction is effectively carried out by tuning the contact interaction to the nucleon mass. The mass of one of the constituent quarks (Q) will be varied while the bare strength of the effective contact interaction is kept constant. For each constituent mass the binding energy of the three-quark system is evaluated. Naturally, this calculation yields the binding energy of the constituent quarks as a function of the baryon ground state mass, because the binding energy and the ground state mass depend only on the mass of the quark Q, with the other inputs kept unchanged.

The binding energy for constituent quarks is a difficult concept to use together with quark confinement which is believed to exist in nature. It is fair to ask, if one has a meaningful model without confinement, how one could extract from the experimental data a quantity to be compared with the model binding energy. This key point will be addressed in detail in the text.

Let us mention that the three-body model with constituent quarks interacting in the light-front with a contact force [7] has been applied to the proton and described its mass, charge radius and electric form factor up to 2 $(\text{GeV}/c)^2$ [8], although the spin was averaged out and before the advent of the $\uparrow\downarrow$ model [5,9]. Recently the same three-quark model was applied to study the dissolution of the nucleon at finite temperature and baryonic density [10].

The paper is organized as follows. In Sec. II, we derive the coupled integral equations for the Faddeev components of the vertex of the three-body light-front bound-state wave function [7], which generalizes the Weinberg-type integral equation found for a two-body bound state [11]. In Sec. III, we present the numerical results for the masses of the
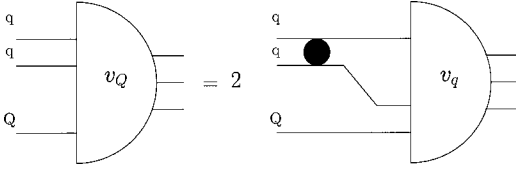
FIG. 1. Diagrammatic representation of Eq. (1). The black bubble represents the two-quark scattering amplitude.

FIG. 2. Diagrammatic representation of Eq. (2). The black bubbles represent the two-quark scattering amplitudes.

nucleon, Λ^0, Λ_c^+ and Λ_b^0, using the flavor independent contact interaction. We show as well how to relate to experimental data the results for the binding energies. Finally, in Sec. IV, we give our conclusions.

II. THREE-QUARK RELATIVISTIC MODEL

The light-front is defined by $x^+ = x^0 + x^3 = 0$ and the coordinates in this space-time hypersurface are given by $x^- = x^0 - x^3$ and $\vec{x}_\perp = (x^1, x^2)$ [2,3]. The coordinate x^+ is recognized as the time and $k^- = k^0 - k^3$, the momentum canonically conjugated, corresponds to the light-front energy. The momentum coordinates k^+ and $\vec{k}_\perp$ are the kinematical momenta canonically conjugated to x^- and $\vec{x}_\perp$, respectively.

A relativistic model for three particles on the light front for a pairwise contact interaction, was derived from the three-body ladder Bethe-Salpeter equation for the Faddeev component of the vertex function, by eliminating the relative x^+ time between the particles [7]. The projection of the covariant dynamics to the light-front hypersurface is performed through the integration over the k^- momentum of the individual particles in the Bethe-Salpeter equation leading to a Weinberg-type equation [11] for three particles. In the work
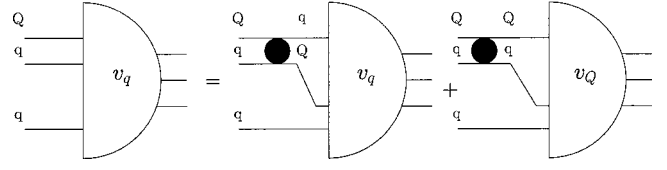
of Ref. [7], in fact the kernel of the Faddeev equation in the light front was derived in lowest order, and in principle corrections of higher order can be systematically constructed following recent discussions [12–14].

Let us sketch the derivation of the light-front Faddeev equations for a heavy-light-light three quark system (Qqq) from the four-dimensional Bethe-Salpeter equations. Two different spectator functions, which correspond to the Faddeev components of the vertex, are possible. For the interacting pair being qq the spectator function is $v_Q(q^\mu)$, function of the four-vector momentum of the quark Q. For the interacting pair Qq the spectator function is $v_q(q^\mu)$. The coupled Faddeev-Bethe-Salpeter equations in the ladder approximation are given by

$$v_Q(q^\mu) = -2\tau_{qq}(M_{qq}^2) \int \frac{d^4k}{(2\pi)^4}$$

$$\times \frac{v_q(k^\mu)}{(k^2 - m_q^2 + \iota\epsilon)[(P_B - q - k)^2 - m_q^2 + \iota\epsilon]}, \quad (1)$$

which is represented diagrammatically in Fig. 1, and

$$v_q(q^\mu) = -\tau_{Qq}(M_{Qq}^2) \int \frac{d^4k}{(2\pi)^4} \left[\frac{v_q(k^\mu)}{(k^2 - m_q^2 + \iota\epsilon)[(P_B - q - k)^2 - m_Q^2 + \iota\epsilon]} + \frac{v_Q(k^\mu)}{(k^2 - m_Q^2 + \iota\epsilon)[(P_B - q - k)^2 - m_q^2 + \iota\epsilon]} \right], \quad (2)$$

which is represented in Fig. 2. The baryon four-momentum is given by P_B, the light and heavy quark masses are m_q and m_Q, respectively. The masses of the virtual two-quark subsystems are $M_{qq}^2 = (P_B - q)^2$ and $M_{Qq}^2 = (P_B - q)^2$ due to conservation of the total four-momentum. The two-quark scattering amplitudes $\tau_{qq}(M_{qq}^2)$ and $\tau_{Qq}(M_{Qq}^2)$ are the solutions of the Bethe-Salpeter equation in the ladder approximation for a contact interaction between the quark pairs, which are derived in detail in the Appendix.

The analytical integration over k^- is performed in Eqs. (1) and (2), using only the pole of the single quark propagator in the lowest half of the complex k^- plane. The pole is given by the on-energy-shell condition $k_{on}^- = (k_\perp^2 + m_\alpha^2)/k^+$,

with $\alpha = q$ or Q when $v_q(k^\mu)$ or $v_Q(k^\mu)$ is integrated, respectively. The condition for a nonvanishing result of the integration in k^- is $0 < k^+ < P_B^+ - q^+$. The spectator functions appearing inside the integrations in Eqs. (1) and (2) depend only on the kinematical momentum, $(k^+, \vec{k}_\perp)$, as long as k_{on}^- is a function of the kinematical momentum. Thus, to close the light-front equations the external momentum is chosen on the k^- shell.

In the rest frame of the baryon of mass M_B, we write that $v_\alpha(q^+, \vec{q}_\perp, q_{on}^-) \equiv v_\alpha(\vec{q}_\perp, y)$, where for convenience the Bjorken momentum fraction $y = q^+/M_B$ is used. The Faddeev equations in the light front written in terms of the kinematical momenta are given by

$$v_Q(\vec{q}_\perp,y) = \frac{i}{(2\pi)^3}\tau_{qq}(M_{qq}^2)\int_0^{1-y}\frac{dx}{x(1-x-y)}\int d^2k_\perp \frac{\theta\!\left(x-\frac{m_q^2}{M_B^2}\right)\theta(k_\perp^{\max}(m_q)-k_\perp)}{M_B^2-\frac{q_\perp^2+m_Q^2}{y}-\frac{k_\perp^2+m_q^2}{x}-\frac{(P_B-q-k)_\perp^2+m_q^2}{1-x-y}}v_q(\vec{k}_\perp,x), \quad (3)$$

$$v_q(\vec{q}_\perp,y) = 2\frac{i}{(2\pi)^3}\tau_{Qq}(M_{Qq}^2)\int_0^{1-y}\frac{dx}{x(1-x-y)}\int d^2k_\perp \left[\frac{\theta\!\left(x-\frac{m_q^2}{M_B^2}\right)\theta(k_\perp^{\max}(m_q)-k_\perp)}{M_B^2-\frac{q_\perp^2+m_q^2}{y}-\frac{k_\perp^2+m_q^2}{x}-\frac{(P_B-q-k)_\perp^2+m_Q^2}{1-x-y}}v_q(\vec{k}_\perp,x)\right.$$

$$\left. +\frac{\theta\!\left(x-\frac{m_Q^2}{M_B^2}\right)\theta(k_\perp^{\max}(m_Q)-k_\perp)}{M_B^2-\frac{q_\perp^2+m_q^2}{y}-\frac{k_\perp^2+m_Q^2}{x}-\frac{(P_B-q-k)_\perp^2+m_q^2}{1-x-y}}v_Q(\vec{k}_\perp,x)\right], \quad (4)$$

where $x=k^+/M_B$. In the first equation of the coupled set, Eq. (3), Q is the spectator quark and qq is the interacting pair. The maximum value for $k_\perp$ is chosen to keep the mass squared of the qq or Qq subsystem real, i.e., $M_{qq}^2\geq 0$ and $M_{Qq}^2\geq 0$, respectively. These constraints in the spectator quark phase space come through the theta functions in the integrations of Eqs. (3) and (4). For $M_{Qq}^2\geq 0$ one has $k_\perp < k_\perp^{\max}(m_q)=\sqrt{(1-x)(M_B^2 x-m_q^2)}$, and $x\geq (m_q/M_B)^2$. For $M_{qq}^2\geq 0$ one has $k_\perp < k_\perp^{\max}(m_Q)=\sqrt{(1-x)(M_B^2 x-m_Q^2)}$, and $x\geq (m_Q/M_B)^2$. For equal particles, Eq. (3) reduces to the one derived in Ref. [7].

Finally, the light-front baryon bound state wave function of the Qqq system in the rest frame is constructed from the Faddeev components of the vertex as in Ref. [8]:

$$\Psi(x_1,\vec{k}_{1\perp};x_2,\vec{k}_{2\perp})$$
$$= \frac{v_q(x_1,\vec{k}_{1\perp})+v_q(x_2,\vec{k}_{2\perp})+v_Q(x_3,\vec{k}_{3\perp})}{\sqrt{x_1 x_2 x_3}(M_B^2-M_0^2)}, \quad (5)$$

where the free three-quark mass M_0^2 is given by

$$M_0^2=\frac{k_{1\perp}^2+m_q^2}{x_1}+\frac{k_{2\perp}^2+m_q^2}{x_2}+\frac{k_{3\perp}^2+m_Q^2}{x_3}. \quad (6)$$

Each constituent quark has momentum fraction x_j and transverse momentum $\vec{k}_{j\perp}$ ($j=1,3$), satisfying $x_1+x_2+x_3=1$ and $\vec{k}_{1\perp}+\vec{k}_{2\perp}+\vec{k}_{3\perp}=0$.

III. RESULTS

The coupled integral equations (3) and (4) for a relativistic system of three constituent quarks with a pairwise zero range interaction are solved numerically. The physical inputs

of the model are the constituent quark masses and the diquark bound state mass. The mass of the ground state baryon (M_B) and the binding energy, $B_B=2m_q+m_Q-M_B$, are calculated. First in this section, before presenting the model results, we provide a qualitative discussion in order to attribute to the low-lying spin 1/2 baryons a binding energy from the experimental data. Then, we compare these data with the model calculations.

A. Qualitative analysis

According to the effective QCD-inspired model calculations of Ref. [6], the low-lying vector mesons are weakly bound systems of constituent quarks while the pseudoscalars are more strongly bound. This justifies our supposition that the masses of the constituent quarks can be derived directly from the vector meson masses:

$$m_u=\frac{1}{2}M_\rho=0.384 \text{ GeV}$$

$$m_s=M_{K*}-\frac{1}{2}M_\rho=0.508 \text{ GeV}$$

$$m_c=M_{D*}-\frac{1}{2}M_\rho=1.623 \text{ GeV} \qquad (7)$$

$$m_b=M_{B*}-\frac{1}{2}M_\rho=4.941 \text{ GeV} ,$$

where the values from Table I are used. Also one can check whether the values of the current quark masses obtained from the constituent ones attain values compatible with the actual knowledge [16]. It is reasonable to think that the constituent quark mass formation mechanism does not distinguish in detail the quark flavor and thus the current quark mass of s, c and b are just given by the difference m_Q^{curr}

TABLE I. Vector (pseudoscalar) meson and current quark masses from Ref. [16]. The estimated values of the current quark masses (last column) are explained in the text. Values quoted in GeV.

Meson		M_M	quark	m_q^{curr} (Ref. [16])	m_q^{curr}
ρ (π)	$u\bar{d}$	0.768 (0.138)	u,d	$(1.5-9)\times10^{-3}$	
K^* (K^+)	$u\bar{s}$	0.892 (0.494)	s	$0.06-0.17$	0.124
D^* (D^0)	$\bar{u}c$	2.007 (1.865)	c	$1.15-1.30$	1.115
B^* (B^+)	$u\bar{b}$	5.325 (5.279)	b	$4-4.4$	4.557

$=m_Q-m_u$ ($Q=s,c,b$). The extracted values of the current masses are quite consistent with the experimental ones from Ref. [16], as one can verify in Table I. At least from this point of view is not unacceptable to define the constituent quark masses from the low-lying vector meson states.

A remark should be added on how ambiguous the qualitative estimates are for the constituent and current quark masses. Errors arise when different meson masses are used as input, and from the current quark masses of the up and down quarks, which we have disregarded, and leads to an error of about 10 MeV. Moreover, another 10 MeV can be attributed to the degeneracy of the ρ and ω mesons in our model. Therefore, we roughly estimate an error of 20 MeV in Table I for our values of current quark masses, and for the constituent quark masses from Eq. (7), as well.

Below, we attribute values to the baryon binding energies, using the constituent quark masses from Eq. (7) and the experimental values of the baryon masses [16]:

$$B_p^{exp}=3m_u-M_p=\frac{3}{2}M_\rho-M_p,$$

$$B_{\Lambda^0}^{exp}=2m_u+m_s-M_{\Lambda^0}=M_{K*}+\frac{1}{2}M_\rho-M_{\Lambda^0},$$

$$(8)$$

$$B_{\Lambda_c^+}^{exp}=2m_u+m_c-M_{\Lambda_c^+}=M_{D*}+\frac{1}{2}M_\rho-M_{\Lambda_c^+},$$

$$B_{\Lambda_b^0}^{exp}=2m_u+m_b-M_{\Lambda_b^0}=M_{B*}+\frac{1}{2}M_\rho-M_{\Lambda_b^0}.$$

The results are presented in Table II.

In Fig. 3, the binding energies of the low-lying pseudo-

TABLE II. Low-lying spin 1/2 baryon experimental masses from Ref. [16] and binding energies from Eq. (8). Values quoted in GeV.

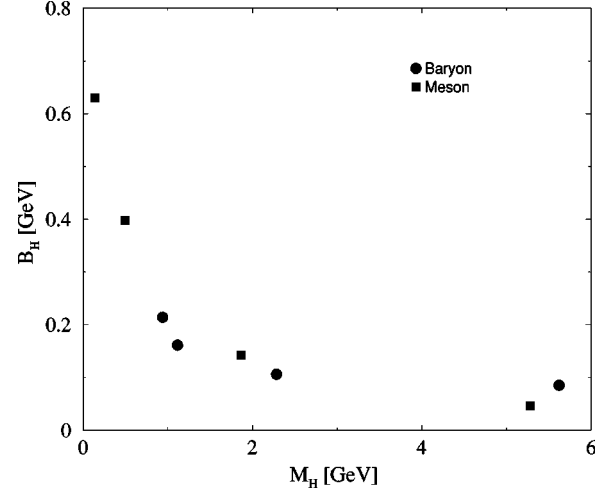| Baryon		$I(J^P)$	M_B	B_B
p	uud	$\frac{1}{2}(\frac{1}{2}^+)$	0.938	0.214
Λ^0	uds	$0(\frac{1}{2}^+)$	1.115	0.161
Λ_c^+	udc	$0(\frac{1}{2}^+)$	2.285	0.106
Λ_b^0	udb	$0(\frac{1}{2}^+)$	5.624	0.085

FIG. 3. Binding energy (B_H) as a function of the mass of the respective low-lying hadron (M_H). Experimental data of pseudoscalar mesons from Table I (full squares). Experimental data of the spin 1/2 baryons from Table II (full circles).

scalar mesons (B_M), defined as the difference between the vector and pseudoscalar masses (see Table I) are plotted against the mass of the corresponding pseudoscalar meson. Also, the values of the binding energies of the spin 1/2 baryons (N, Λ^0, Λ_c^+ and Λ_b^0) from Eq. (8) are shown as a function of the corresponding baryon mass. We observe a smooth trend in the plot of Fig. 3 for B_M as well as for B_B as a function of the hadron ground state mass. The increase of the heavy quark mass produces the same qualitative behavior irrespective of the nature of the hadron, being a meson or a baryon.

The data for mesons shown in Fig. 3, was described by the effective QCD-inspired model once the hypothesis of the flavor independence of the interaction was adopted [6]. This is consistent with the fundamental QCD theory in which the gluon does not recognize flavor but color [1]. Figure 3 suggests that for baryons, it is reasonable to assume, as a first guess, that the constituent quark interaction would be flavor independent.

B. Model calculations

The physical input of the light-front model defined by the coupled integral equations (3) and (4) are the constituent quark masses and the diquark bound state mass. Up to this point the masses of the constituent quarks have been defined by Eq. (7). The value of the diquark mass has to be found. The diquark mass was fitted to the value of the proton mass, with a given constituent quark mass by the solution of Eq. (3) with $q=Q=u$. We use $m_u=0.386$ GeV which together with the nucleon mass of 0.938 GeV implies $M_d=0.695$ GeV. The slightly different m_u in respect to the one found in Eqs. (7) is just adequate to the value obtained in Ref. [8], where the above quark mass was used with a reasonable description of the proton charge radius and electric form factor below $2(\text{GeV}/c)^2$.

We solve the coupled equations (3) and (4) for fixed $m_u=0.386$ GeV and $M_d=0.695$ GeV and different values of
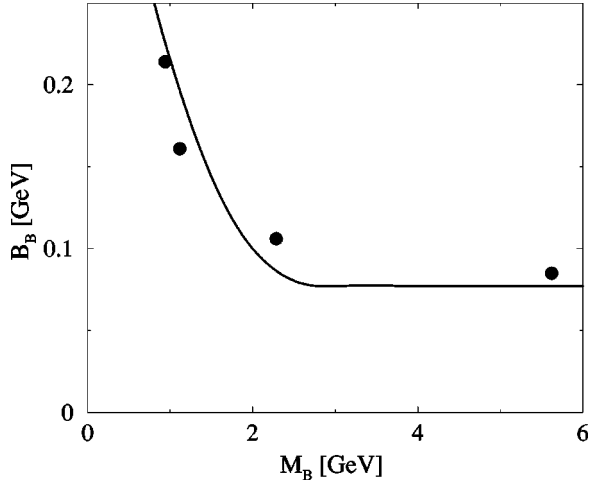
FIG. 4. Binding energy of the low-lying spin 1/2 baryon states as a function of the respective ground state mass of the baryon. The results of the light-front Faddeev model calculation are shown by the solid line. Full circles are the data from Table II for the nucleon, Λ^0, Λ_c^+ and Λ_b^0.

m_Q. Thus, the binding energy for the spin 1/2 baryons Λ^0, Λ_c^+ and Λ_b^0 are obtained by changing the value of m_Q ($Q=s,c,b$). Each value of m_Q produces a ground state mass and binding energy. In Fig. 4, instead of showing the binding energy as a function of m_Q, we plot it as a function of the ground state mass in a continuous curve and compare with the attributed experimental values. For the baryon mass above 2.3 GeV, the bound Qqq system goes to the diquark threshold. This gives the saturation value of 0.077 GeV seen in Fig. 4. The model calculation with a flavor independent effective interaction is able to reproduce the trend of the attributed experimental binding energies as a function of the mass of the baryon ground state. In view of the simplicity of the model, the agreement between the binding energies obtained theoretically with the attributed experimental values is quite reasonable.

Our present results, although, in a simplified model generalize the flavor independent effective interaction of the QCD-inspired $\uparrow\downarrow$ model to the context of the dynamics of constituent quarks forming the baryon. The very existence of the smooth pattern shown in Figs. 3 and 4, for the correlation between binding and masses, tells us that the dominant physics is the mass variation of the constituent quark and the spin effects should average out. Taking into account that spin degree of freedom is averaged out in the model and at the same time the reasonable description of the data is found in Fig. 4, gives us the confidence that the main physics related to quark mass variation is reasonable described by the flavor independent contact interaction.

IV. CONCLUSIONS

We have studied the binding of the constituent quarks forming the low-lying spin 1/2 baryonic states of the nucleon, Λ^0, Λ_c^+ and Λ_b^0. We use a relativistic three-quark model of the baryon defined on the light front, where the inputs were the constituent quark masses and the diquark
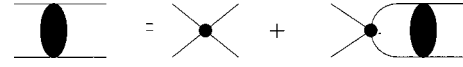

FIG. 5. Bethe-Salpeter equation in ladder approximation for the two quark-scattering amplitudes from Eq. (A1). The contact interaction is represented by the dot.

mass in the light sector. The effective interaction was chosen of a contact form and spin was averaged out. The contact interaction includes the minimal number of physical scales to describe these baryons. Recently in a QCD-inspired model of mesons, in addition to the contact interaction, motivated by the hyperfine interaction between the quarks, a Coulomb-like potential was considered as well. Going beyond the hyperfine interaction itself, the zero range interaction mimics those aspects of QCD that bind the constituent quarks in the meson, which in this paper was used to build the baryon. We observed a surprising reproduction of the trend and magnitude of the binding energies as a function of the distint quark mass. Our conclusion, while unexpected, still carries a more detailed analysis which includes the quark spin and the Coulomb-type interaction. The results shown here give a support for the extension of the QCD-inspired model of Refs. [5,6] to baryons.

As the feature we addressed here is valid irrespective of the composite hadron nature, we think that our conclusion of the flavor dependence of baryonic masses may still hold in a more realistic model. However, we have to stress that the present model is based on the notion of constituent quarks, and it only uses the constituent quark mass which, in fact, because spin effects are averaged, does not really enter into spin dependent interactions in our calculations. When spin dependent interactions are present, constituent quark models can lead to conflict with data, as has been shown in Ref. [17] for the proton spin measured in deep inelastic scattering. Therefore, the extension of our conclusion for the case that spins are no longer averaged has to be cautious to avoid conflict with spin data.

APPENDIX: TWO-QUARK SCATTERING AMPLITUDE

The two-body scattering amplitudes $\tau_{qq}(M_{qq}^2)$ and $\tau_{Qq}(M_{Qq}^2)$ are the solutions of the Bethe-Salpeter equations in the ladder approximation, represented diagrammatically in Fig. 5, for a contact interaction between the quarks [7,15]. In this case the solution is just given by the infinite sum of the product of "bubble" diagrams (Fig. 6) multiplied by powers of the bare interaction strength. The result is given by the geometrical series,

$$\tau_{\alpha q}(M_{\alpha q}^2) = \frac{1}{i\lambda^{-1} - \mathcal{B}_{\alpha q}(M_{\alpha q}^2)}, \tag{A1}$$

FIG. 6. "Bubble" diagram representing Eq. (A2).

where $\alpha = q$ or Q and λ is the bare interaction strength. The function $\mathcal{B}_{\alpha q}(M_{\alpha q}^2)$ is the "bubble" diagram represented in Fig. 6,

$$\mathcal{B}_{\alpha q}(M_{\alpha q}^2) = \int \frac{d^4k}{(2\pi)^4} \frac{i}{(k^2 - m_q^2 + i\varepsilon)}$$

$$\times \frac{i}{[(P_{\alpha q} - k)^2 - m_\alpha^2 + i\varepsilon]}, \qquad (A2)$$

where the total four-momentum of the quark pair is $P_{\alpha q}$ with $P_{\alpha q}^2 = M_{\alpha q}^2$.

The four-dimensional integration in Eq. (A2) is performed in light-front variables. First, the virtual propagation of the intermediate quarks is projected at equal light-front times [7,12], by analytical integration over k^- in the momentum loop. The non-zero contribution to Eq. (A2) comes from $0 < k^+ < P_{\alpha q}^+$ for $P_{\alpha q}^+ > 0$,

$$\mathcal{B}_{\alpha q}(M_{\alpha q}^2) = \frac{i}{2(2\pi)^3} \int \frac{dk^+ d^2 k_\perp}{k^+ (P_{\alpha q}^+ - k^+)}$$

$$\times \frac{\theta(P_{\alpha q}^+ - k^+)\theta(k^+)}{P_{\alpha q}^- - \frac{k_\perp^2 + m_q^2}{k^+} - \frac{(P_{\alpha q} - k)_\perp^2 + m_\alpha^2}{(P_{\alpha q}^+ - k^+)}}.$$

$$(A3)$$

Now, we introduce the invariant quantity $x = k^+/P_{\alpha q}^+$ and the relative momentum

$$\vec{K}_\perp = (1-x)\vec{k}_\perp - x(\vec{P}_{\alpha q} - \vec{k})_\perp,$$

in Eq. (A3), which gives

$$\mathcal{B}_{\alpha q}(M_{\alpha q}^2) = \frac{i}{2(2\pi)^3} \int \frac{dx \, d^2 K_\perp}{x(1-x)}$$

$$\times \frac{\theta(1-x)\theta(x)}{M_{\alpha q}^2 - \frac{K_\perp^2 + (m_\alpha^2 - m_q^2)x + m_q^2}{x(1-x)}}. \qquad (A4)$$

The function $\mathcal{B}_{\alpha q}(M_{\alpha q}^2)$ has a log-type divergence in the transverse momentum integration. The renormalization

$\tau_{\alpha q}(M_{\alpha q}^2)$ is done by taking into account the physical information of the interacting light-quark pair system, that we suppose has a bound state. Using this physical condition to define the two-quark scattering amplitude we have studied the nucleon in the three-quark light-front model [8]. This model fitted, simultaneously, the proton mass, the charge radius and the electric form factor below 2 $(\text{GeV}/c)^2$ [8]. Here, we just use the same renormalization condition.

The pole of the light-quark scattering amplitude, $\tau_{qq}(M_{qq}^2)$ is found when M_{qq} is equal to the mass of the bound qq pair, M_d. Thus, the bound state pole of the scattering amplitude demands that

$$i\lambda^{-1} = \mathcal{B}_{qq}(M_d^2), \qquad (A5)$$

which is enough to render finite the scattering amplitudes τ_{qq} and τ_{Qq}. Thus, the bare strength of the effective contact interaction between the constituent quarks q and Q does not depend on flavor. In this manner, we extend the flavor independence of the gluon interaction of the fundamental QCD Lagrangian to the effective interaction.

The final equation for the two-quark scattering amplitude is

$$\tau_{\alpha q}(M_{\alpha q}^2) = \frac{1}{\mathcal{B}_{qq}(M_d^2) - \mathcal{B}_{\alpha q}(M_{\alpha q}^2)}. \qquad (A6)$$

The log-type divergence of $\tau_{\alpha q}$ is removed by the subtraction in Eq. (A6).

In particular, the analytical form of Eq. (A6) is [7]

$$\tau_{qq}(M_{qq}^2) = -i(2\pi)^2 \left\{ \sqrt{\frac{m_q^2}{M_d^2} - \frac{1}{4}} \right.$$

$$\times \arctan\left(\frac{1}{2\sqrt{\frac{m_q^2}{M_d^2} - \frac{1}{4}}} \right) - \sqrt{\frac{m_q^2}{M_{qq}^2} - \frac{1}{4}}$$

$$\left. \times \arctan\left(\frac{1}{2\sqrt{\frac{m_q^2}{M_{qq}^2} - \frac{1}{4}}} \right) \right\}^{-1}, \qquad (A7)$$

for $0 < M_{qq} < 2m_q$, which is enough for the integration in Eq. (3).

[1] C. Itzykson and J.-B. Zuber, *Quantum Field Theory* (McGraw-Hill, New York, 1987).

[2] S.J. Brodsky, H.-C. Pauli, and S.S. Pinsky, Phys. Rep. **301**, 299 (1998).

[3] J. Carbonell, B. Desplanques, V. Karmanov, and J.-F. Mathiot, Phys. Rep. **300**, 215 (1998).

[4] R.J. Perry, A. Harindranath, and K.G. Wilson, Phys. Rev. Lett. **65**, 2959 (1990).

[5] H.-C. Pauli, in *New Directions in Quantum Chromodynamics*, edited by C.R. Ji and D.P. Min (AIP, Melville, NY, 1999), pp. 80–139; Nucl. Phys. B (Proc. Suppl.) **90**, 154 (2000); **90**, 259 (2000).

[6] T. Frederico and H.-C. Pauli., Phys. Rev. D **64**, 054007 (2001).

[7] T. Frederico, Phys. Lett. B **282**, 409 (1992); S.K. Adhikari, L. Tomio, and T. Frederico, Ann. Phys. (N.Y.) **235**, 77 (1994).

[8] W.R.B. Araújo, J.P.B.C. de Melo, and T. Frederico, Phys. Rev. C **52**, 2733 (1995).

[9] H.-C. Pauli, Eur. Phys. J. C **7**, 289 (1998).

[10] S. Matiello, M. Beyer, T. Frederico, and H.-J. Weber, Phys. Lett. B **251**, 33 (2001).

[11] S. Weinberg, Phys. Rev. **150**, 1313 (1966).

[12] J.H.O. Sales, T. Frederico, B.V. Carlson, and P.U. Sauer, Phys. Rev. C **61**, 044003 (2000); **63**, 064003 (2001).

[13] J.R. Cooke, G.A. Miller, and D. Phillips, Phys. Rev. C **61**, 064005 (2000).

[14] M. Mangin-Brinet and J. Carbonell, Phys. Lett. B **474**, 237 (2000).

[15] J.P.B.C. de Melo, A.E.A. Amorim, L. Tomio, and T. Frederico, J. Phys. G **27**, 1031 (2001).

[16] Particle Data Group, D. Groom *et al.*, Eur. Phys. J. C **15**, 1 (2000).

[17] K. Suzuki and W. Weise, Nucl. Phys. **A634**, 141 (1998).